Microbial colonisation of transparent glass-like carbon films triggered by a reversible radiation-induced hydrophobic to hydrophilic transition

Blanca Jalvo, Javier Santiago-Morales, Pablo Romero, Roberto Guzman de Villoria & Roberto Rosal, Microbial colonisation of transparent glass-like carbon films triggered by a reversible radiation-induced hydrophobic to hydrophilic transition, RSC Adv., 6, 50278-50287, 2016,

http://dx.doi.org/10.1039/C6RA04960E

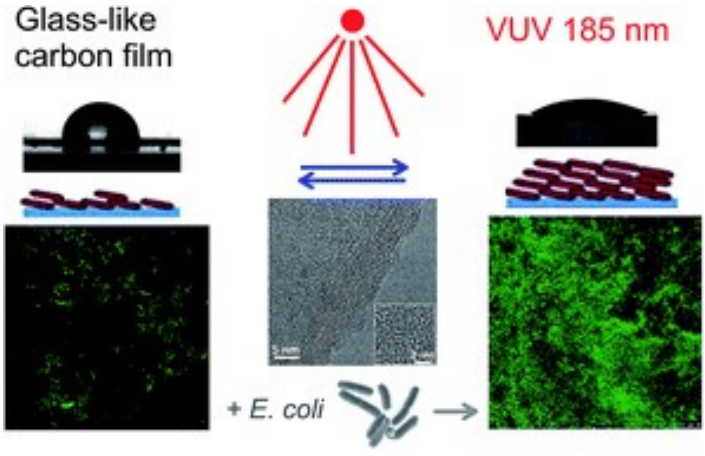

Microbial colonisation of transparent glass-like carbon films triggered by a reversible radiation-induced hydrophobic to hydrophilic transition

Blanca Jalvo[1], Javier Santiago-Morales[1], Pablo Romero[2], Roberto Guzman de Villoria[2], Roberto Rosal[1,3,*]

[1] Department of Chemical Engineering, University of Alcalá, E-28871 Alcalá de Henares, Madrid, Spain
[2] Madrid Institute for Advanced Studies of Materials (IMDEA Materials Institute), Tecnogetafe, E-28906, Madrid, Spain
[3] Madrid Institute for Advanced Studies of Water (IMDEA Agua), Parque Científico Tecnológico, E-28805, Alcalá de Henares, Madrid, Spain

* Corresponding author: roberto.rosal@uah.es

Abstract

We report a reversible wettability hydrophobic to hydrophilic transition in transparent glass-like carbon films under ultraviolet irradiation when the source emitted in the vacuum ultraviolet. The transition occurred at doses below 5 J/cm^2 for devices emitting at 185 nm and was absent when using a 266 nm monochromatic laser source. Hydrophilicity, measured as the water contact angle, was higher when the films were irradiated in air with high relative humidity. Sample hydrophobicity was almost entirely restored over the following 24 h and was completely restored to the initial when samples were sotred for sufficient time under ambient conditions. Our observations were consistent with a transition caused by the dissociative adsorption of water molecules leading to the formation of polar surface groups. Over the few hours in which the surface remained hydrophilic under ambient conditions, a rapid colonisation with *Escherichia coli* took place with extensive biofilm formation. The percent surface colonised increased from 1.30 % ± 0.4 % to a maximum of 51.0 % ± 2.7 % for carbon films irradiated in dry air. Irradiation in the presence of water vapour led to surfaces wihch were more hydrophilic, but less prone to bacterial adhesion. Bacterial colonisation was favoured in films with intermediate hydrophilicity irrespective of the surface charge, measured as the zeta potential. Our study demonstrates that vacuum ultraviolet irradiation induces a wettability transition in glass-like carbon films, and that a relatively short ultraviolet dose of 185 nm irradiation render their surfaces highly biocompatible.

Keywords: Glass-like carbon films, reversible wettability, ultraviolet irradiation; bacterial colonisation; surface hydrophilicity

1. Introduction

Controlling cell-material interactions is essential in many expanding applications such as the production of antimicrobial surfaces or biocompatible materials. It has been shown that surface topography and physicochemical properties determine cell adhesion and proliferation[1,2]. The adhesion of microorganisms on natural or synthetic surfaces is a critical issue in many important fields, such as the fight against human infections and pathogen control during food processing and storage[3,4]. Microbial adhesion is detrimental when associated with the dissemination of pathogens, but can be also beneficial, for example for the production of wastewater treatment bioreactors or for biopolymer degradation[5]. Once attached to a surface, bacteria form biofilms consisting of cells immobilised cells embedded in a polymeric matrix of microbial origin. Biofilms are complex biological communities characterised by cells with an altered phenotype that create their own environment[6]. The prevention of biofilms and the enhancement of biocompatibility are closely interconnected goals that require a deep understanding of surface physicochemistry[7].

Tailoring hydrophilicity has been shown to be important in a range of biomedical uses, such as the creation of nano-bio interfaces for molecular medicine[8]. These applications usually require surface modifications that enhance hydrophilicity in order to allow cellular attachment and growth, and these are frequently accomplished by decoration with chemical functionalities such as hydroxyl or carboxylic acid groups[9]. Particular attention has been paid to systems in which a reversible hydrophobic-hydrophilic transition is triggered by external stimuli such as electrical potential or irradiation[10,11]. Several materials display reversible wettability upon ultraviolet (UV) irradiation. In particular, metal oxides switch between hydrophobicity and hydrophilicity due to the adsorption of water molecules that photodissociate to generate surface hydroxyl groups[12].

Several carbon-based materials also display reversible hydrophobic-hydrophilic transition. Graphene undergoes switching between hydrophobic and hydrophilic states upon application of an electric field, which reduces the energy barrier for dissociative adsorption of water[13]. The reversible wettability transition of carbon nanotube films upon UV exposure has been attributed to the formation of hydrophilic groups upon chemisorption of oxygen[11]. Graphene also becomes temporarily hydrophilic when irradiated[14,15]. These results suggest that hydrophilicity could be induced by the dissociative adsorption of oxygen or water molecules[14,15]. A similar behaviour of graphene oxide has been attributed to reversible deoxygenation of the graphene oxide surface[16]. This phenomenon is largely, but not entirely superficial, as it has been shown that surface modification of graphene is only independent on substrate properties in films of more than about six layers[17].

Molecular-scale understanding and manipulation of the wetting behaviour of carbon-based surfaces is still unclear and poses fundamental and practical challenges[18,19]. In this study, we investigated the influence of a radiation-induced wetting transition on the bacterial colonisation of a carbonaceous surface using a strain of the opportunistic bacteria *E. coli* and assessing irradiation-triggered surface biocompatibility and biofilm formation. Furthermore, we examined an aspect that has received insufficient research attention to date, namely the spectral distribution of ultraviolet radiation using well-defined sources. Although it is well known that conventional low-pressure mercury-vapour 254 nm lamps emit a significant fraction of their power in the vacuum ultraviolet, this fact is generally overlooked in the literature. We used glass-like carbon films, which belong to a family of disordered carbons such as diamond-like or glassy carbon films, for which no data have been reported to date. In this regard, disordered carbons are easier to produce and manipulate than monolayer graphene, and consequently their use in real applications would be more feasible.

2. Experimental

Synthesis of the carbon film. A commercial copper foil was used as catalyst for chemical vapour deposition (CVD) of carbon films (100µm-thick copper foil, 99.8 % purity, Sigma Aldrich) following a process similar to that used to produce CVD graphene[20]. Pristine copper foils were cut into pieces measuring 22 x 50 mm^2 and cleaned in a pure ethanol ultrasound bath for 10 minutes. The foils were then air-dried. We used a custom-made CVD reactor consisting of a longitudinal mobile tubular furnace that allowed fast heating/cooling rates[21], and three gas lines (Ar, H_2 and C_2H_4) connected to a 22 mm diameter quartz tube. First, the lines were flushed with Ar to displace the air inside the tube, maintaining the copper foil outside the furnace heating zone. Then, the furnace was heated to the synthesis temperature (850 °C) with a flow of 1000/20 sccm Ar/H_2, maintaining the sample outside the heating zone. Once the temperature had stabilised, the furnace was rapidly moved (*ca*. 3s) to situate the centre of the heating zone exactly in the copper foil position. Annealing was performed for 10 min with 1000/20 sccm of Ar/H_2. A gas mixture of 500/20/20 sccm of $Ar/H_2/C_2H_4$ was used in the next step for carbon film synthesis, which took 5 min. Finally, the furnace was moved back away from the sample to enable rapid cooling under an argon flow. Further details on the experimental procedure for producing carbon films can be found elsewhere[22].

Carbon film transfer. During the CVD process, a carbon film of ca. 5 nm thick was deposited on top of the copper foil. Next, the carbon film was transferred to a thin polymer film following conventional PMMA-assisted transfer[23,24]. First, the carbon film/copper was gently flattened using two clean glass holders. Three drops of a PMMA solution (495PMMA A Resists, Microchem) were homogeneously distributed on top of the carbon film/copper using a laboratory weighing paper to level the liquid PMMA solution. We waited for two hours to allow the solvent to evaporate and then repeated the process two more times. Once the PMMA had dried under ambient conditions, the PMMA/carbon film/copper sandwich structure was placed in a $FeCl_3$–HCl copper etching solution (Sigma Aldrich 667528) with the PMMA face-down. After 2 h, the copper etchant was replaced with a fresh one, and etching continued for a further 24 h. Copper etchant was cleaned 5 times with deionised water and the sample was maintained in a deionised water bath for 24 h. After the cleaning process, PMMA/films were recovered with glass holders. We did not remove the PMMA, but used it as a support for the carbon films to perform the experiments described below. The 22 x 50 mm^2 sample was cut into slices with a stainless steel blade (approximately 10 x 15 mm), and these were submerged in new deionised water and placed on cover glasses (0.13-0.16 mm thickness, Labbox) with the carbon film facing up and the PMMA in contact with the cover glass. The samples were dried in a vacuum oven at 50 °C for 2 h.

Physical characterisation of carbon films. As synthesised carbon film on copper foil was dipped in $FeCl_3$–HCl copper etching solution (Sigma Aldrich, 667528) and detached in the form of flakes, which were cleaned several times with deionised water. The carbon flakes were then transferred onto a thermal oxide wafer (300 nm SiO_2 on Si) for both atomic force microscopy (AFM) and Raman measurements. AFM characterisation and details of surface topography details are described in the Supplementary Information. Raman spectra of the carbon film were collected from the top of the wafers (Jasco, NRS-5100). At least three measurements per synthesis condition were taken, using a Nd:YAG green laser (532 nm, aperture: 4000 µm,

grating: 1800 l/mm, slit: 200×1000 µm, resolution: 7.42 cm^{-1}), with two accumulations of 20 s exposure in a range of 1000–3250 cm^{-1} (laser power 5.3 mW). We compared the Raman spectra of our carbon films with monolayer graphene on a silicon wafer (Graphenea). Lastly, several carbon flakes were transferred onto a copper grid for analysis under a transmission electron microscope (JEOL JEM 3000F). The results are presented in Figure 1. The carbon films were composed of semicontinuous curved crystallites of about 5 nm in an amorphous carbon matrix (Figure 1a), which resembled the curved graphene fragments that form glass-like carbons[25,26]. The Raman spectra, which are compared to monolayer graphene in Figure 1b, revealed a certain degree of disorder due to an the increase in D peak at 1350 cm^{-1}, G band broadening, the presence of a D″ band (*ca.* 1100 cm^{-1}) and additional peaks at about 1240 and 1480 cm^{-1}[27]. The combination of these modes produced the D+D″ band at 2450 cm^{-1} and D+D′ at 2950 cm^{-1}. D and D′ overtones at 2D 2700 cm^{-1} and 2D′ at 3250 cm^{-1} also broadened in disordered graphites[28,29].

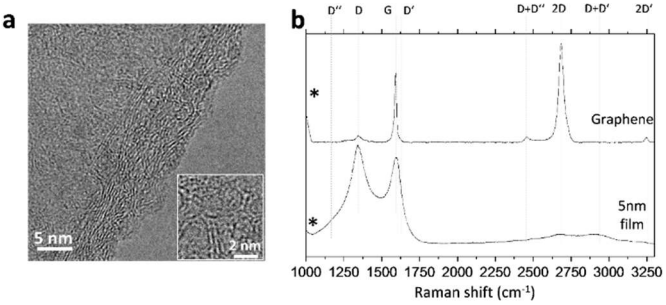

Figure 1. Transmission electron micrograph of a 5-nm-thick carbon film (a) and Raman spectra of CVD glass-like carbon films compared to monolayer graphene (b).

Irradiation. UV irradiation of glass-like carbon films was performed at 20 °C. Prior to irradiation, carbon films were heated at 50 °C for 2h under a vacuum of 10 kPa). The equipment used for irradiating carbon films was as follows. (1) A 15 W Heraeus Noblelight TNN 15/32 low-pressure mercury vapour lamp emitting at 254 nm with a secondary peak at 185 nm. This lamp uses synthetic quartz, which is transparent to the vacuum ultraviolet emission at 185 nm (5 % of the radiant power). Using hydrogen peroxide actinometry, we determined that lamp irradiance was 18.7 mW cm^{-2}. (2) A Vilber-Lourmat Bio-Link BLX-254 Crosslinker equipped with 5 x 8 W 254 nm T-8C lamps. These lamps are "ozone-free", meaning that the quartz they are made of absorbs most of the 185 nm emission line. Irradiance at 15 cm, in the lower part of the chamber, was 820 µW cm^{-2}. (3) An FQSS 266-200 diode pumped passively Q-switched solid-state laser (CryLas, Germany) emitting pulses (< 1.5 ns) at 266 nm > 200 µJ at 20 MHz. The irradiance for a given set of conditions was determined by means of a LOT-Oriel LSZ014 radiant power meter with a spectral range of 0.19 to 25 µm connected to a Gentec-EO Tuner monitor. To investigate the effects of humidity, a sufficient amount of distilled water at 85 °C was placed in the UV chamber or in a structure enclosing the irradiation space, which made it possible to maintain ~80 % RH throughout the experiment. In all cases, the temperature was maintained at 20 °C ± 2 °C. At least 5 min preconditioning was applied before irradiation.

Contact angle measurements and surface free energy. Carbon films wettability was tested as soon as possible after irradiation employing an optical contact angle meter (Krüss DSA25 Drop Shape Analysis System) at room temperature using the sessile drop technique. To measure bacterial hydrophobicity, bacterial surfaces for measuring contact angles were prepared by collecting bacterial cells on a cellulose acetate filter (pore diameter, 0.45 µm, MicronSep Cellulosic, Thomas Scientific) to a density of 10^8 cells per mm^2. Filters with a continuous bacterial layer were mounted on glass slides and dried for 15 to 60 min. Then, we measured the contact angle of drops of purified water on the bacterial surface. No change in contact angle occurred between 15 and 60 min. Samples were placed on the test cell and drops of purified water, glycerol and diiodomethane were gently deposited on the surfaces using a built-in delivery syringe. Contact angle measurements for each surface were taken at 20 °C in at least three different positions for each solvent.

The Lifshitz–van der Waals (LW), electron donor (−) and electron acceptor (+) components of the surface tension were estimated from CA values for water, glycerol and diiodomethane according to the following expression in which the free energy of interaction between a solid, S, and a liquid, L, can be obtained from pure liquid contact angles, θ[30]:

$$\Delta G_{SL} = -(1+\cos\theta)\,\gamma_L = -2\left(\sqrt{\gamma_S^{LW}\gamma_L^{LW}} + \sqrt{\gamma_S^{+}\gamma_L^{-}} + \sqrt{\gamma_S^{-}\gamma_L^{+}}\right) \quad (1)$$

In this approach, the total surface free energy (γ) is the sum of the non-polar Lifshitz-van der Waals component (γ^{LW}) and the acid-base component (γ^{AB}), which in turn comprises two non-additive parameters: the electron-acceptor (γ^{+}) and the electron-donor (γ^{-}) surface tension parameters. Eq. (1) contains the three components of the solid surface free energy, γ_S^{LW}, γ_S^{+} and γ_S^{-}, as unknowns, which can be solved by measuring the CA with three liquids. The components of the liquid surface free energy, γ_L^{LW}, γ_L^{+} and γ_L^{-}, for the probe liquids are available in the literature for a number of pure substances[31].

According to Van Oss, the total interfacial tension between the solid film and water, γ_{SL}, can be expressed as follows[32]:

$$\gamma_{SL} = \left(\sqrt{\gamma_S^{LW}} - \sqrt{\gamma_L^{LW}}\right)^2 + 2\left(\sqrt{\gamma_S^{+}\gamma_S^{-}} + \sqrt{\gamma_L^{+}\gamma_L^{-}} - \sqrt{\gamma_S^{+}\gamma_L^{-}} - \sqrt{\gamma_L^{+}\gamma_S^{-}}\right) \quad (2)$$

In addition, the free energy of interaction between two identical surfaces, S, immersed in a liquid, L, is:

$$\Delta G_{SLS} = -2\gamma_{SL} \quad (3)$$

The energy of interaction, ΔG_{SLS}, gives a direct measure of the hydrophobicity or hydrophilicity of the surface. When $\Delta G_{SLS} > 0$, the surface is hydrophilic, and when $\Delta G_{SLS} < 0$, it is hydrophobic.

Zeta potential measurements. Surface zeta potential was measured via electrophoretic light scattering (DLS, Malvern Zetasizer Nano ZS) and using the surface zeta potential cell (ZEN 1020) from Malvern. In brief, a rectangular section no larger than 7 mm x 4 mm was glued onto the sample holder using Araldite adhesive. The cell was inserted into a disposable plastic 10 mm square cuvette containing 1.2 mL of 10 mM KCl (pH 7.0) aqueous solution, with 0.5 % (w/w) polyacrylic acid (450 kDa) as a tracer (a negatively charged tracer is required for negatively charged surfaces). Measurements were performed at 25 °C at six different displacements from the sample surface, which enabled the surface zeta potential to be calculated by Zetasizer software. The pH was adjusted using 1M KOH and 1 M HCl.

Bacterial strains and bioassays. *E.coli* cells (CECT 516) were grown overnight at 37 °C in nutrient agar medium (for 1 L solution in distilled water: 5 g beef extract, 10 g peptone, 5 g NaCl and for solid media 15 g agar powder with pH adjusted to 7.2), while shaking. After reactivation, cell density was tracked by measuring optical density (OD) at 600 nm. Exponentially growing cultures on nutrient medium were diluted to an OD_{600} of 0.04, and 150 µL was placed on a carbon film inside 24-well polystyrene plates and incubated for 18 h at 30 °C without shaking. After incubation and liquid culture removal, films were carefully washed with distilled water.

The Live/Dead BacLight Bacterial Viability Kit (Molecular Probes, Invitrogen Detection Technologies, Carlsbad, CA, USA) was used to evaluate bacterial viability. Under live/dead staining all cells exhibit green fluorescence (SYTO 9), whereas nonviable bacterial cells display red fluorescence (Propidium iodide, PI) with dye uptake depending upon cell membrane integrity. Films were stained with 10 µL BacLight stain (a mixture of SYTO 9 and PI in DMSO) according to the manufacturer's recommendations, and incubated in the dark for 15 min at room temperature. For matrix visualisation, biofilms were also stained with 200 µL Film Tracer SYPRO Ruby Biofilm Matrix Stain (Molecular Probes, Invitrogen) per film, incubated in the dark for 30 min at room temperature, and then rinsed with distilled water. After incubation, films were transferred to a glass slide, covered with a glass cover slip and sealed. All images were acquired at 18 h after inoculation in the microdevice using a Leica Microsystems Confocal SP5 fluorescence microscope (Leica Microsystems, Germany). For green fluorescence (SYTO 9), excitation was performed at 488 nm (Ar) and emission was recorded at 500-575nm. For red fluorescence (PI, dead cells), the excitation/emission wavelengths were 561 nm (He-Ne) and 570-620 nm, respectively. For SYPRO Ruby Biofilm Matrix Stain the excitation/emission wavelengths were 450 nm and 610 nm respectively.

A modification of Fletcher's method was used for biofilm quantification[33]. Approximately 200 µL of a crystal violet 0.1 % solution was extended over the washed film surface and incubated for 15 min in order to stain adhered cells. Excess stain was eliminated by rinsing with water. Plates were air-dried and 1 mL of 95 % ethanol was added to each well in order to extract crystal violet from cells. Destaining was performed overnight while gently shaking. Lastly, the dye was measured at OD_{590}. Measurements were taken three times for each experimental condition.

3. Results and discussion

Wettability and the effect of radiation sources. Reversible hydrophobic-hydrophilic transition of transparent glass-like carbon films was achieved using UV irradiation from three different sources: (1) a low-pressure mercury lamp emitting at 254 nm with a secondary peak at 185 nm, representing about 5 % of the radiant power; (2) a crosslinker chamber equipped with "ozone-free" lamps, which have a tube that absorbs most of the 185 nm emission line and (3) a diode pumped solid-state laser emitting pulses at 266 nm. Low-pressure mercury vapour lamps emitting VUV light of 185 nm can photolyse water molecules into hydrogen atoms and hydroxyl radicals. Ozone-free lamps also have this capacity, although weaker. The reason for using multiple irradiating devices was to determine the effect of vacuum ultraviolet (VUV) water-splitting emission, which is usually overlooked. The laser emits pure 266 nm without any line in the vacuum ultraviolet (VUV), while sources (1) and (2) have high and residual 185 nm lines, respectively.

Figure 2 shows the effect of irradiation at different UV doses on the water CA measured in transparent glass-like carbon films. Each sample was preconditioned under vacuum (10 kPa, 50 °C) for 2 h prior to irradiation. A set of samples were measured at 30 % ± 5 % RH, identified in what follows as "dry" conditions. A parallel set of films were irradiated under wet air (80 % ± 5 % RH), which was obtained by placing cups containing water at 85 °C into the irradiation space. In this case, carbon films were preconditioned under wet air for at least 10 min before irradiation. Water CA decreased upon irradiation from 99.0° ± 3.4° up to 22.8° ± 2.5°, which was the lowest CA obtained and corresponded to films irradiated with the 185+254 nm low-pressure mercury lamp. When using the 185-254 lamp, water CA initially decreased sharply from pre-irradiation values until stabilising after 4-5 min. The decrease in hydrophobicity was much slower when using the irradiation chamber, taking about 8 hours to reach a plateau. No significant effect was observed for

irradiation using the 266 nm solid-state laser. The differences obtained for this device were essentially within the boundaries of experimental error. Water CA for the 185+254 lamp reached considerably lower values than those obtained using the irradiation chamber. The difference between the synthetic quartz VUV emitting lamp and the "ozone free" irradiation of the chamber amounted to ~23° in wet air. It is noteworthy that with UV doses of 5 or 25 J/m^2, the hydrophobic states changed to hydrophilic ones depending on whether the irradiation was performed with the low-pressure mercury lamp or the irradiation chamber.

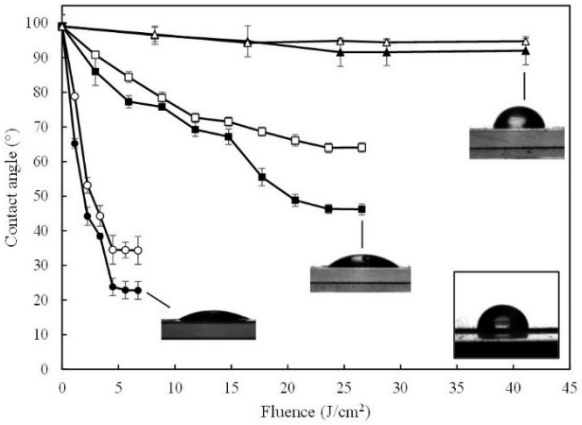

Figure 2. Water contact angles of transparent glass-like carbon films for different irradiation devices and UV doses. Low-pressure mercury lamp (○, ●), irradiation chamber (□, ■), laser (△, ▲). Empty symbols: dry air (~ 30 % RH), filled symbols: wet air (~ 80 % RH). Inset at the bottom right: glass-like carbon after vacuum treatment and before irradiation.

After reaching maximum hydrophilicity, corresponding to the water CA plateau shown in Figure 2, glass-like carbon films were stored under laboratory conditions (1 atm, 20 °C) to investigate the recovery of hydrophobicity. The results are shown in Figure 3, where zero time represents the end of irradiation and the first measurement was performed after 1 h. During the first 24 h following irradiation, the samples recovered most of their hydrophobicity, with contact angle values increasing up to the 81°-89° range. After 24 h, all samples displayed a water CA > 90°, close to the values of non-irradiated carbon films. The water CA of irradiated samples could be completely restored to the initial level by storing samples for sufficient time under ambient conditions.

The CA values for water, glycerol and diiodomethane are shown in Table 1. In the case of bacteria, the measurements were performed on bacterial lawns deposited on cellulose acetate filters as described elsewhere[34]. The surface zeta potential was determined using the surface zeta potential cell described above and measuring the particle mobility of a tracer at several distances away from the surface. Figure 4 shows the surface zeta potential values for glass-like carbon films, vacuum preconditioned glass-like carbon, and samples irradiated in low and high RH air with the lamp and the irradiation chamber. In all cases, the surfaces were negatively charged, with the highest negative value corresponding to dry-irradiated samples (-54 mV) irrespective of the irradiation device. Samples irradiated in wet air reached a surface potential of -47 mV, whereas non-irradiated carbon films displayed a zeta potential of -41 mV. Although small, these differences were statistically significant, and could be due to the absorption of ultraviolet radiation by water molecules along the path.

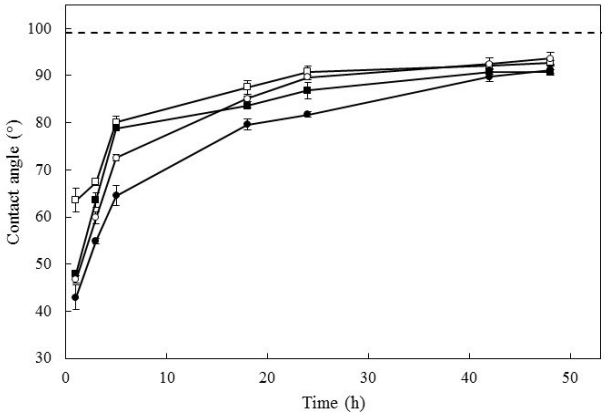

Figure 3. Evolution of water contact angles of irradiated glass-like carbon films for different times under ambient conditions. Low-pressure mercury lamp (○, ●), irradiation chamber (□, ■), laser (△, ▲). Empty symbols: dry air (~ 30 % RH), filled symbols: wet air (~ 80 % RH).

Table 1. Surface characterization by means of contact angle measurements

surface	θ_{water}	$\theta_{glycerol}$	$\theta_{diiodomethane}$
gC	82.3 ± 0.3	80.0 ± 3.3	44.4 ± 2.4
gC + vacuum*	97.7 ± 3.0	83.9 ± 3.7	36.3 ± 3.1
gC irradiated (dry)**	36.1 ± 0.5	68.6 ± 0.6	67.8 ± 1.3
gC irradiated (wet)**	23.6 ± 2.4	62.6 ± 3.2	68.0 ± 1.8
E. coli	16.7 ± 1.3	44.0 ± 3.5	58.7 ± 0.5

* 2 h, 50 °C, 10 kPa
** Lamp 185+254 nm, 5 min.

Wettability transition in irradiated amorphous carbon materials has been considered a consequence of changes in surface topography. Carbon films have been shown to display important differences in wettability, switching from hydrophilicity to super-hydrophobicity, determined by a combination of morphology and carbon state features[18]. Work performed with carbon nanotube films suggests that oxygen chemisorption would lead to hydrophilic surface moieties, such as hydroxyl groups, which are mainly located at lattice defects[35]. Water molecules would physically adsorb at these sites, preferentially filling the apertures in rough surfaces, which results in a reduced water contact angle. The surface can even reach a superhydrophilic state.

Reversibility can be explained by desorption of surface water, which is gradually replaced by oxygen molecules[11]. The induction of surface defects by irradiation or other treatments has been proposed as a starting point for dissociative adsorption of water and for inducing wettability transition in graphene films[14]. Carbon nanotube films reach superhydrophilicity, whereas graphene and amorphous carbon films, including those used in this study, give rise to moderately hydrophilic surfaces. The differing extent of hydrophilicity obtained during the treatment of different materials could be a consequence of the varying surface roughness of the irradiated materials. Carbon nanotube films, which exhibit multiscale surface roughness, can become superhydrophilic, whereas smoother surfaces such as graphene and amorphous carbon films yield moderately hydrophilic surfaces.

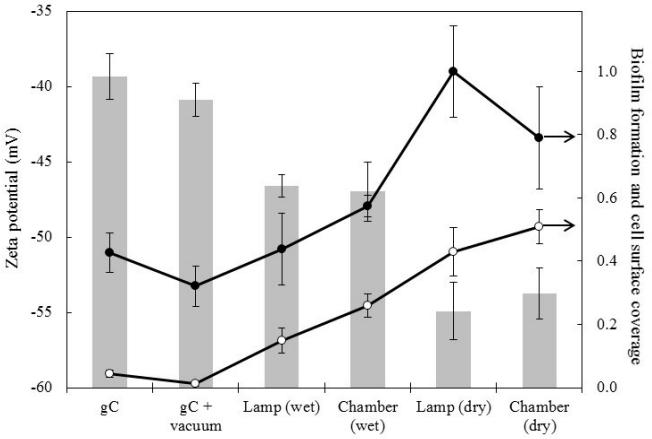

Figure 4. Surface zeta potential (bars, expressed in mV), bacterial colonisation (lines) measured using the crystal violet method in units relative to their maximum value (lamp irradiation in dry air, •) and fractional surface coverage by metabolically active bacteria (from live/dead staining, ○).

The wettability transition for graphene has been simulated using Raman spectroscopy, suggesting that the dissociative adsorption of water could take place on a graphene surface under 254 nm irradiation[15]. However, the first gas-phase O-H bond scission, corresponding to the formation of the radicals HO and H, amounts to 497.1 kJ/mol or 5.15 eV[36]; consequently, the VUV line at 185 nm (6.70 eV) can split the water molecule, but the 254 nm UV-C radiation, equivalent to 4.88 eV, cannot dissociate it. On the other hand, the energy barrier for the dissociative adsorption of water on graphene is 3.455 eV, after which HO and H move to sites on top of carbon atoms, yielding a final structure that gives rise to an energy release of 0.921 eV. Because of this, the total energy balance for the dissociative adsorption of water on a graphene surface is 2.534 eV[13]. Therefore, it is energetically possible that interaction with a carbon sp2 surface will enable 254 nm radiation to split water, but it is not clear whether the transition could actually take place using monochromatic radiation because the experiments performed to date have used 185 nm emitting lamps[14,15].

Our irradiation devices made it possible to determine the effect of 185 nm irradiation. The rapid increase in wettability under lamp (185+254 nm) irradiation and the complete lack of effect of the 266 nm solid-state laser setup (Figure 2) together suggest a determining role of VUV emission in creating hydroxyl radicals from water. These hydroxyl radicals would interact with the carbon film surface giving rise to the hydrophilic moieties responsible for the lower water CA of irradiated samples. Previous results have shown that an oxygen-rich environment does not enhance the hydrophilic transition, indicating that the oxidation of carbon atoms or vacancies by ozone produced upon VUV irradiation does not take place[15]. In addition, the reverse of the dissociative adsorption of water on carbon surface is energetically favoured, which is compatible with the reversible wettability transition observed in this study for glass-like carbon films (Figure 3) and in graphene by others[14,15].

Table 2. Surface energy components of glass-like carbon films and bacteria (mJ/m^2)

surface	γ_S^{LW}	γ_S^+	γ_S^-	γ_S^{AB}	γ_S	ΔG_{SLS}
gC	35.4	0.02	5.8	0.7	36.2	-55.1
gC+vacuum*	39.6	0.02	0	0.1	39.7	-100.5
gC irradiated (dry)**	23.4	0	69.0	0	24.6	64.7
gC irradiated (wet)**	23.9	0.01	82.2	1.3	24.6	80.5
E. coli	29.4	1.5	63.2	19.1	48.5	43.4

* 2 h, 50 °C, 10 kPa
** Lamp 185+254 nm, 5 min.

CA values provided information about the hydrophobicity of surfaces. For non-irradiated glass-like carbon films, water CA was always > 80°, indicating a relatively hydrophobic surface. Upon irradiation, CA dropped to 20°-40° indicating a hydrophilic nature. In agreement with previously published data, the surface of *E. coli* cell lawns was clearly hydrophilic[37]. Table 2 gives the values of surface energy components for irradiated and non-irradiated films and bacterial lawns. The value observed for total solid-liquid interfacial energy, γ_S, was 39.7 mJ/m^2 for vacuum preconditioned glass-like carbon films. This figure is relatively close to the surface energy reported for graphene, 46.7 mJ/cm^2, and lower than the 54.8 mJ/cm^2 and 62.1 mJ/m^2 reported for graphite and graphene oxide, respectively[38]. However, surface free energies for graphene are somewhat controversial. Kozbial et al. reported 53.0-63.8 mJ/m^2 (depending on the model used) with values fluctuating with the adsorption of airborne hydrocarbons and the wetting transparency effect[39].

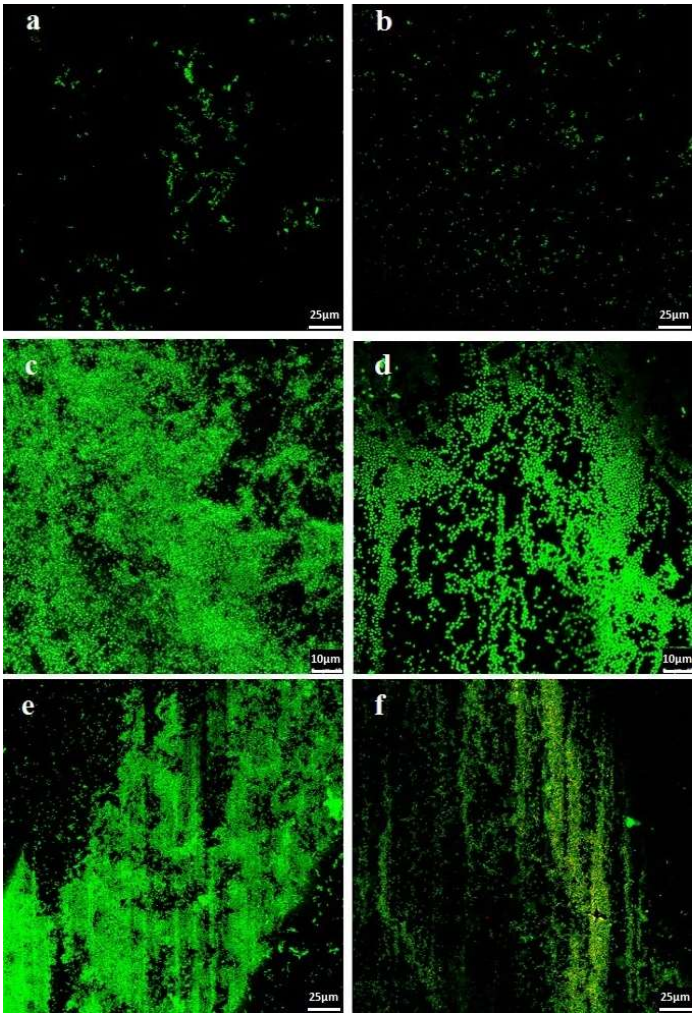

Figure 5. Live/dead confocal micrographs of *E. coli* cultured on (a) glass-like carbon film as produced, (b) vacuum preconditioned film, (c) chamber-irradiated films in dry air, (d) chamber-irradiated films in wet air, (e) lamp-irradiated films in dry air, (f) lamp-irradiated films in wet air.

Hydrophilicity and microbial growth on glass-like carbon surfaces. Figure 5 gives the results for live/dead bacterial viability staining. The images correspond to representative confocal micrographs of glass-like carbon films in contact with *E. coli* cultures for 18 h. The high growth rate of bacteria on irradiated surfaces was particularly clear for samples irradiated in dry air (Figures 5c and 5e). Conversely, non-irradiated carbon films were essentially free of bacteria (Figures 5a and 5b). It is interesting to note that some red-stained, nonviable bacteria appear on the lamp-irradiated film in wet air (Figure 5f). Quantitative results were obtained by counting green pixels (viable bacteria) in digitally treated images with the aid of the public domain Java image processing software ImageJ. The percent surface colonised by bacteria (Figure 4) was 1.30 % ± 0.4 % in vacuum preconditioned carbon films, which increased to 51.0 % ± 2.7 % (chamber, dry air), 25.9% ± 1.8 % (chamber, wet air), 42.9 % ± 3.8 % (lamp, dry air) and 14.8 ± 2.0 % (lamp, wet air).

Figure 6 shows SEM micrographs of *E. coli* cultured on different substrates, which essentially present the same behaviour, with extensive colonisation of glass-like carbon samples irradiated in dry air. Vacuum preconditioned film was almost free of bacterial growth (Figure 6a), but a high amount of bacteria was clearly observed colonising the films irradiated in dry air (Figures 6c and 6d) and, to a lesser extent, on films irradiated in wet air (Figure 6b).

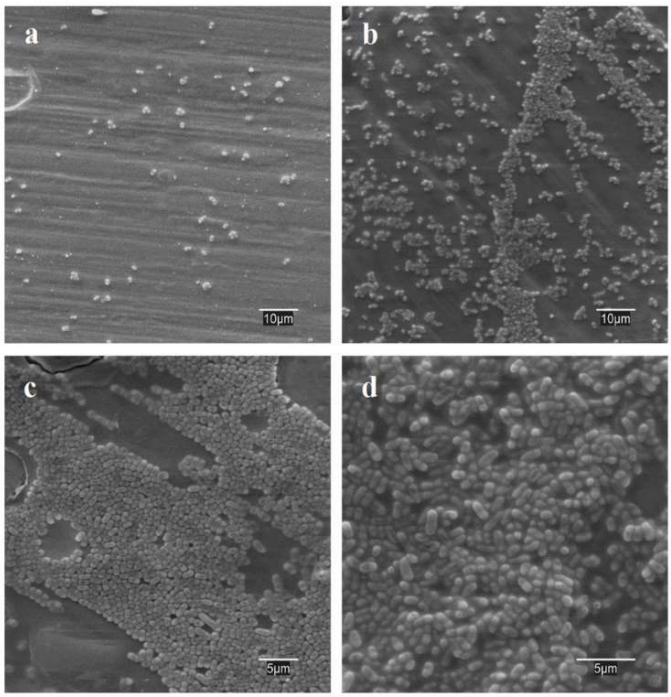

Figure 6. SEM images of *E. coli* cultured on (a) vacuum preconditioned film, (b) lamp-irradiated films in wet air, (c) chamber-irradiated films in dry air and (d) lamp-irradiated films in dry air.

The formation of an extracellular polymeric matrix was visualised using the FilmTracer SYPRO Ruby biofilm matrix stain. This stain labels most classes of proteins, including lipoproteins, porins and enzymes, which, among others, are found in the extracellular polymeric matrix of biofilms[40]. As with many other bacteria, *E. coli* tend to form biofilms consisting of cells immobilised at a substratum and embedded in an organic polymer matrix offering protection against hostile environments. The matrix also offers the possibility of intercellular communication, allowing rapid up- and down-regulation of gene expression and thus favouring adaptive strategies. The results of FilmTracer staining are shown in Figure S2 (Supplementary Information) as confocal micrographs. The extensive formation of biofilms is apparent in samples irradiated in dry air (Figures S2c and 2e), whereas they are almost absent from non-irradiated films and scarce in those irradiated in wet air.

It has been shown that hydrophobic interactions play a dominant role in the adhesion of *E. coli* strains irrespective of lipopolysaccharide composition or cell charge[41]. They are responsible for the orientation of the water molecules adsorbed on the surfaces, which in turn determines the repulsion between surfaces[42]. If a

surface is weakly polar, the most closely adsorbed water molecules are not rigidly oriented and another surface can approach under the influence of Lifshitz-van der Waals forces. It is interesting to note that rather than repelling water, a hydrophobic surface attracts water, although with less energy binding than hydrophilic surfaces[43]. Therefore, the hydrophobic interaction between two non-polar bodies in water is the result of the hydrogen-bonding energy of cohesion of the water molecules surrounding them. The consequence is that maximum interaction can be expected between two surfaces when the difference in hydrophilicity is not too great. Otherwise, adsorbed water molecules would lead to a net repulsion force.

Table 2 shows the ΔG_{SLS} values obtained by computing the hydrophilicity of bacteria and glass-like carbon films. Clearly, carbon films were hydrophobic as received and upon heating in vacuum their hydrophobicity increased to -100 mJ/m^2. Irradiation renders carbon films more hydrophilic, particularly when these are irradiated in wet air. The electron donor component of the surface energy corresponding to irradiated samples is clearly high, with the highest value corresponding to carbon films treated in wet air. This is consistent with the scenario depicted previsouly in which water molecules split into hydrogen and hydroxyl radicals, giving rise to oxygenated groups in surface carbon atoms. The data also show that the *E. coli* strain was highly hydrophilic and a predominantly electron donor (high value of γ_S^-). The bacterial strain and glass-like carbon irradiated in dry air displayed the closest ΔG_{SLS} values, whereas for wet air irradiation, the carbon surface became considerably more hydrophilic. The energy of interaction, ΔG_{SLS}, closely agrees with the extent of bacterial colonisation as shown in Figures 4 to 6 and in Figure S2: the higher the similarity of ΔG_{SLS} with that of *E. coli*, the greater the bacterial growth observed.

As a rule, hydrophobic bacteria adhere on hydrophobic surfaces, whereas hydrophilic microorganisms attach to hydrophilic surfaces; however, bio-surface interactions are somewhat more complex. First, the thermodynamic approach assumes direct contact between bacteria and surface, creating a new interface, but the presence of cell appendages, such as pili and flagella renders direct contact quite unrealistic[7]. On the other hand, solid surfaces exposed to culture media comprise complex interfaces with a number of adsorbed organic and inorganic compounds, which modify the way in which microorganisms adhere and complicate the use of simple physicochemical models[44]. In fact, the free energy of adhesion calculated from surface energy components is usually unsatisfactory because of the strong influence exerted by the growth medium used when culturing microorganisms, which has a significant impact on bacterial adhesion[45].

The other physicochemical factor affecting bacterial adhesion is surface charge, which we measured as surface zeta potential (Figure 4). All surfaces were negatively charged with a zeta potential ranging from -40.9 ± 1.1 mV for vacuum preconditioned films to -54.9 ± 1.9 mV for carbon irradiated in dry air. The negative charge of carbon films is due to the presence of oxygen-containing groups associated with sp3 hybridised carbon atoms at edges and defects. Such chemical functionalities, which include epoxy, hydroxyl and carboxylic groups, give rise to a negative charge in liquids with a high dielectric constant, such as water[46]. Irradiation increased the negative charge, as expected from the hydroxyl radical-driven formation of oxygenated functional surface groups explained previously. Moieties such as epoxide or carbonyl are responsible for polar surface properties, whereas carboxyl and hydroxyl groups are responsible for their negative charge[47,48]. Electrostatic repulsion could be expected to play a role in bacterial adhesion, given the negative surface charge of bacterial outer membranes: the zeta potential of *E. coli* is approximately -30 mV[41]. However, the data show that the more negatively charged surfaces were more prone to bacterial colonisation as revealed by crystal violet (Figure 4) and live/dead staining (Figures 4 and 5) and SEM imaging (Figure 6). In all cases, dry-irradiated films were more easily colonised than the more hydrophilic ones irradiated in wet air. The more negative surface charge did not protect the surface from bacterial attachment. This is consistent with the secondary role played by electrostatic interactions during bacterial adhesion noted by other authors[49].

Bacterial colonisation is a complex process which with bacterial adhesion to the substrate and continues with the formation of biofilms. Ruby FilmTracer images acquired after 18 h in contact with *E. coli* cultures (Figure S2) revealed a protein network of extracellular substances responsible for the mechanical stability of biofilms. They also showed extensive biofilm formation on irradiated surfaces of glass-like carbon film, indicating that colonisation proceeded easily on hydrophilic films, but an excessively hydrophilic surface, such as that obtained during irradiation in wet air, was relatively resistant to biofilm formation. Once formed, the biofilm constitutes a substrate in itself, and from then on, the characteristics of the underlying surface become less important for microbial growth. Reversibility of the hydrophilic-hydrophobic transition does not imply biofilm detachment because the polymeric matrix mediates between surface and cells forming a cohesive and three-dimensional network that is very difficult to remove[50].

4. Conclusions

In conclusion, we have shown that UV irradiation triggers the transition from a hydrophobic to hydrophilic surface in transparent glass-like carbon

films. The effect took place with doses below 5 J/cm^2 using irradiation devices emitting at 185 nm, and was not observed in sources free from vacuum ultraviolet. The transition was reversible, and the water contact angle was essentially restored during the first 24 h under ambient conditions following irradiation. The hydrophilic transition is attributed to the dissociative adsorption of water molecules yielding oxygenated surface moieties. Carbon films were highly susceptible to bacterial colonisation and biofilm formation during the period in which they were hydrophilic. Up to 50 % of the surface of glass-like carbon films irradiated in dry air (~ 30 % RH) became covered by *E. coli* in the 18 h following inoculation. Irradiation in more humid air (~ 80 % RH) led to more hydrophilic surfaces, which were less prone to bacterial adhesion, indicating that bacterial colonisation took place preferentially on films with intermediate hydrophilicity values, whereas the higher energy of interaction associated with more hydrophilic surfaces resulted in a lower affinity for bacteria. Surface charge, always negative, did not play a significant role. These results are relevant for applications that require enhanced or suppressed biocompatibility of carbonaceous graphene-like materials.

Acknowledgements

This work has been financed by the Dirección General de Universidades e Investigación de la Comunidad de Madrid, Research Network 0505/AMB-0395 and the Spanish Ministry of Science (CTM2013-45775). One of the authors, JSM, would like to thank the University of Alcalá for the award of a postdoctoral grant.

References

1 D. Aronov, R. Rosen, E.Z. Ron, G.Rosenman. Tunable hydroxyapatite wettability: effect on adhesion of biological molecules. *Process Biochem.* 2006, **41**, 2367-2372.

2 K. Anselme, P. Davidson, A.M. Popa, M. Giazzon, M. Liley, L. Ploux. The interaction of cells and bacteria with surfaces structured at the nanometre scale. *Acta Biomaterialia* 2010, **6**, 3824-3846.

3 R.J. Emerson, T.A. Camesano. Nanoscale investigation of pathogenic microbial adhesion to a biomaterial. *Appl. Environ. Microbiol.* 2004, **70**, 6012-6022.

4 E.A. Araújo, N.J. de Andrade, L.H.M. da Silva, A.F. de Carvalho, C.A. de Sá-Silva A.M. Ramos. Control of microbial adhesion as a strategy for food and bioprocess technology. *Food Bioprocess. Tech.* 2010, **3**, 321-332.

5 R. Bos, H.C. van der Mei, H.J. Busscher. Physico-chemistry of initial microbial adhesive interactions—its mechanisms and methods for study. *FEMS Microbiol. Rev.* 1999, **23**, 179-230 (1999).

6 M.E. Shirtliff, J.T. Mader, A.K. Camper. Molecular interactions in biofilms. *Chem. Biol.* 2000, **9**, 859–871.

7 K. Hori, S. Matsumoto. Bacterial adhesion: From mechanism to control. *Biochem. Eng. J.* 2010, **48**, 424–434.

8 D. Sahni, A. Jea, J.A. Mata, D.C. Marcano, A. Sivaganesan, J.M. Berlin, C.E. Tatsui, Z. Sun, T.G. Luerssen, S. Meng, T.A. Kent, J.M. Tour. Biocompatibility of pristine graphene for neuronal interface. J. *Neurosurg. Pediatr.* 2013, **11**, 575-583.

9 Y. Wang, Z. Li, J. Wang, J. Li, Y. Lin. Graphene and graphene oxide: biofunctionalization and applications in biotechnology. *Trends Biotechnol.* 2011, **29**, 205–212.

10 N. Verplanck, E. Galopin, J.C. Camart, V. Thomy, Y. Coffinier, R. Boukherroub. Reversible electrowetting on superhydrophobic silicon nanowires. *Nano Lett.* 2007, **7**, 813-817.

11 J. Yang, Z. Zhang, X. Men, X. Xu, X. Zhu. Reversible superhydrophobicity to superhydrophilicity switching of a carbon nanotube film via alternation of UV irradiation and dark storage. *Langmuir* 2010, **26**, 10198-10202.

12 S. Wang, X. Feng, J. Yao, L. Jiang. Controlling Wettability and Photochromism in a Dual-Responsive Tungsten Oxide Film. *Angew. Chem. Int. Ed.* 2006, **45**, 1264-1267.

13 Q.G. Jiang, Z.M. Ao, D.W. Chu, Q. Jiang. Reversible transition of graphene from hydrophobic to hydrophilic in the presence of an electric field. *J. Phys. Chem. C* 2016, **116**, 19321-19326.

14 X. Zhang, S. Wan, J. Pu, L. Wang, X. Liu, X. Highly hydrophobic and adhesive performance of graphene films. *J. Mater. Chem.* 2011, **21**, 12251–12258.

15 Z. Xu, Z. Ao, D. Chu, A. Younis, C.M. Li, S. Li. Reversible hydrophobic to hydrophilic transition in graphene via water splitting induced by UV irradiation. *Sci. Rep.* 2014, **4**, 6450.

16 J. Rafiee, X. Mi, H. Gullapalli, A.V. Thomas, F. Yavari, Y. Shi, P.M. Ajayan, N.A. Koratkar. Wetting transparency of graphene. *Nat. Mater.* 2012, **11**, 217-222.

17 S.B. Bon, M. Piccinini, A. Mariani, J.M. Kenny, L. Valentini. Wettability and switching of electrical conductivity in UV irradiated graphene oxide films. *Diam. Relat. Mat.* 2011, **20**, 871–874.

18 Y. Zhou, B. Wang. X. Song, E. Li, G. Li, S. Zhao, H. Yan. Control over the wettability of amorphous carbon films in a large range from hydrophilicity to super-hydrophobicity. *Appl. Surf. Sci.* 2006, **253**, 2690–2694.

19 Y. Zhou, B. Wang, X. Zhang, M. Zhao, E. Li, H. Yan. The modifications of the surface wettability of amorphous carbon films. *Colloid. Surf. A Physicochem. Eng. Asp.* 2009, **335**, 128-132.
20 X. Li, W. Cai, J. An, S. Kim, J. Nah, D. Yang, R. Piner, A. Velamakanni, I. Jung, E. Tutuc, S.K. Banerjee, L. Colombo, R.S. Ruoff. Large-Area Synthesis of High-Quality and Uniform Graphene Films on Copper Foils. *Science* 2009, **324**, 1312-1314.
21 P. Romero, R. Oro, M. Campos, J.M. Torralba, R. Guzman de Villoria. Simultaneous synthesis of vertically aligned carbon nanotubes and amorphous carbon thin films on stainless steel. *Carbon* 2015, **82**, 31–38.22
22 P. Romero, P. A. Postigo, E. Baquedano, J. Martinez, A. Bosca, R. Guzman de Villoria, Controlled synthesis of nanocrystalline glass-like carbon thin films with tuneable electrical and optical properties. *Chem. Eng. J.*, in press: doi:10.1016/j.cej.2016.04.005.
23 A. Reina, X. Jia, J. Ho, D. Nezich, H. Son, V. Bulovic, M.S. Dresselhaus, J. Kong. Large area, few-layer graphene films on arbitrary substrates by chemical vapor deposition. *Nano Lett.* 2009, **9**, 30–35.
24 W. Cai, Y. Zhu, X. Li, R.D. Piner, R.S. Ruoff. Large area few-layer graphene/graphite films as transparent thin conducting electrodes. *Appl. Phys. Lett.* 2009**, 95**, 123115.
25 P.J.F. Harris. New Perspectives on the Structure of Graphitic Carbons. *Crit. Rev. Solid State Mater. Sci.* 2005, **30**, 235–253.
26 P.J.F. Harris. Fullerene-related structure of commercial glassy carbons. *Philos. Mag.*, 2004, **84**, 3159–3167.
27 A.C. Ferrari, J. Robertson. Interpretation of Raman spectra of disordered and amorphous carbon. *Phys. Rev. B* 2000, **61**, 14095.
28 P. May, M. Lazzeri, P. Venezuela, F. Herziger, G. Callsen, J.S. Reparaz, A. Hoffmann, F. Mauri, J. Maultzsch. Signature of the two-dimensional phonon dispersion in graphene probed by double-resonant Raman scattering. *Phys. Rev. B* 2013, **87**, 075402.
29 A.C. Ferrari, D.M. Basko. Raman spectroscopy as a versatile tool for studying the properties of graphene. *Nat. Nanotechnol.* 2013, **8**, 235–246.
30 C.J. Van Oss, M.K. Chaudhury, R.J. Good. Interfacial Lifshitz-van der Waals and Polar Interactions in Macroscopic Systems. *Chem. Rev.* 1988, **88**, 927-941.
31 A. Holländer, A. On the selection of test liquids for the evaluation of acid-base properties of solid surfaces by contact angle goniometry. *J. Colloid Interface Sci.* 1995, **169**, 493-496.
32 C.J. Van Oss. Development and applications of the interfacial tension between water and organic or biological surfaces. *Colloids Surf. B: Biointerfaces* 2007, **54**, 2–9.
33 M. Fletcher. The effects of culture concentration and age, time, and temperature on bacterial attachment to polystyrene. *Can. J. Microbiol.* 1977, **23**, 1-6.
34 H.J. Busscher, A.H. Weerkamp, H.C. van der Mei, A.W.J. van Pelt, H.P. de Jong, J. Arends. Measurement of the surface free energy of bacterial cell surfaces and its relevance for adhesion. *Appl. Environ. Microbiol.* 1984, **48**, 980-983.
35 T. Savage, S. Bhattacharya, B. Sadanadan, J. Gaillard, T.M. Tritt, Y.P. Sun, Y. Wu, S. Nayak, R. Car, N. Marzari, P.M. Ajayan, A.M. Rao. Photoinduced oxidation of carbon nanotubes. *J. Phys. Condens. Matter*, 2003, **15**, 5915-5921.
36 B. Ruscic, A.F. Wagner, L.B. Harding, R.L. Asher, D. Feller, D.A. Dixon, K.A. Peterson, Y. Song, X. Qian, C.Y. Ng, J. Liu, W. Chen, D.W. Schwenke. On the enthalpy of formation of hydroxyl radical and gas-phase bond dissociation energies of water and hydroxyl. *J. Phys. Chem. A* 2002, **106**, 2727-2747.
37 D. Aronov, R. Rosen, E.Z. Ron, G. Rosenman. Electron-induced surface modification of hydroxyapatite-coated implant. *Surf. Coat. Technol.* 2008, **202**, 2093-2102.
38 S. Wang, Y. Zhang, N. Abidi, L. Cabrales. Wettability and surface free energy of graphene films. *Langmuir* 2009, **25**, 11078-11081.
39 A. Kozbial, Z. Li, C. Conaway, R. McGinley, S. Dhingra, V. Vahdat, F. Zhou, B. D'Urso, H. Liu, L. Li. Study on the surface energy of graphene by contact angle measurements. *Langmuir* 2014, **30**, 8598-8606.
40 M.P. Nandakumar, A. Cheung, M.R Marten. Proteomic analysis of extracellular proteins from *Escherichia coli* W3110. *J. Proteome Res.* 2006, **5**, 1155-1161.
41 Y.L Ong, A. Razatos, G. Georgiou, M.M. Sharma. Adhesion forces between *E. coli* bacteria and biomaterial surfaces. *Langmuir* 1999, **15**, 2719-2725.
42 C.J. Van Oss. Hydrophobicity and hydrophilicity of biosurfaces. *Curr. Opin. Colloid Interface Sci.* 1997, **2**, 503-512.
43 C.J. Van Oss. Hydrophobicity of biosurfaces - origin, quantitative determination and interaction energies. *Colloids Surf. B Biointerfaces* 1995, **5**, 91-110.
44 M.G. Brading, J. Jass, H.M. Lappin-Scott. Dynamics of bacterial biofilm formation. In: *Microbial Biofilms*; Lappin-Scott, H.M., Costerton J.W., Eds.; Cambridge University Press, Cambridge, 1995, pp 46–63.
45 Q .Zhao, Y. Liu, C. Wang, S. Wang. Evaluation of bacterial adhesion on Si-doped diamond-like

carbon films. *Appl. Surf. Sci.* 2007, **253**, 7254-7259.
46 S.M. Notley, R.J. Crawford, E.P. Ivanova. Bacterial Interaction with Graphene Particles and Surfaces. In: *Advances in Graphene Science*, M. Aliofkhazraei, Ed.; InTech, 2013 (DOI: 10.5772/56172)
47 I. Dékány, R. Krüger-Grasser, A. Weiss. Selective liquid sorption properties of hydrophobized graphite oxide nanostructures. *Colloid Polym. Sci.* 1998, **276**, 570-576.
48 K. Haubner, J. Murawski, P. Olk, L.M. Eng, C. Ziegler, B. Adolphi, E. Jaehne. The route to functional graphene oxide. *ChemPhysChem* 2010, **10**, 2131-2139.
49 J. Wang, N. Huang, P. Yang, Y.X. Leng, H. Sun, Z.Y. Liu, P.K. Chu. The effects of amorphous carbon films deposited on polyethylene terephthalate on bacterial adhesion. *Biomaterials* 2004, **25**, 3163-3170.
50 H.C. Flemming, J. Wingender. The biofilm matrix. *Nat. Rev. Microbiol.* 2010, **8**, 623-633.

Supplementary information

Microbial colonisation of transparent glass-like carbon films triggered by a reversible radiation-induced hydrophobic to hydrophilic transition

Blanca Jalvo[1], Javier Santiago-Morales[1], Pablo Romero[2], Roberto Guzman de Villoria[2] and Roberto Rosal[1,3,*]

[1] Department of Chemical Engineering, University of Alcalá, 28871 Alcalá de Henares, Madrid, Spain
[2] Madrid Institute for Advanced Studies of Materials (IMDEA Materials Institute), Tecnogetafe, E-28906, Madrid, Spain
[3] Madrid Institute for Advanced Studies of Water (IMDEA Agua), Parque Científico Tecnológico, E-28805, Alcalá de Henares, Madrid, Spain

*roberto.rosal@uah.es

Contents

Atomic force microscopy measurements. Surface topography of the carbon film was analyzed by atomic force microscopy (AFM) using a Park XE150 apparatus. The images were acquired in non-contact mode using a non-contact cantilever (PPP-NCHR, Park System) with a tip set point of about ~30-40 nm and amplitudes between ~25-45 nm and a scan rate of 0.50Hz. The images (512 x 512 pixels and areas of 10 μm^2 and 2 μm^2) were processed and analyzed using XEI software (version 1.7.1). A comparison of AFM scans before treatment (Figures S1 a, c, e and g) and UV treated samples in the same areas showed globular and vermicular features appearing after both dry (Figures S1 b and f) and wet (Figures S1 d and h) irradiation. Some of the cavities of non-irradiated samples almost disappeared. A deeper analysis showed that the globular and vermicular features detected after UV treatments derived from surface features presented in the carbon film/PMMA composite PMMA transfer (Figures S1e and f). These features seemed to swell and smooth their edges because of the irradiation. UV treatment in wet air seems to show smoother and more swollen features than those irradiated in dry air. We analyzed the surface features of the copper foil treated with the same synthesis conditions (850 °C) but without ethylene, to avoid carbon film synthesis. The results showed that copper foil developed roughness in the form of small domes of about 300 nm, which were transferred to the carbon film/PMMA composite as cavities of approximately the same size (Figures S1 g and h).

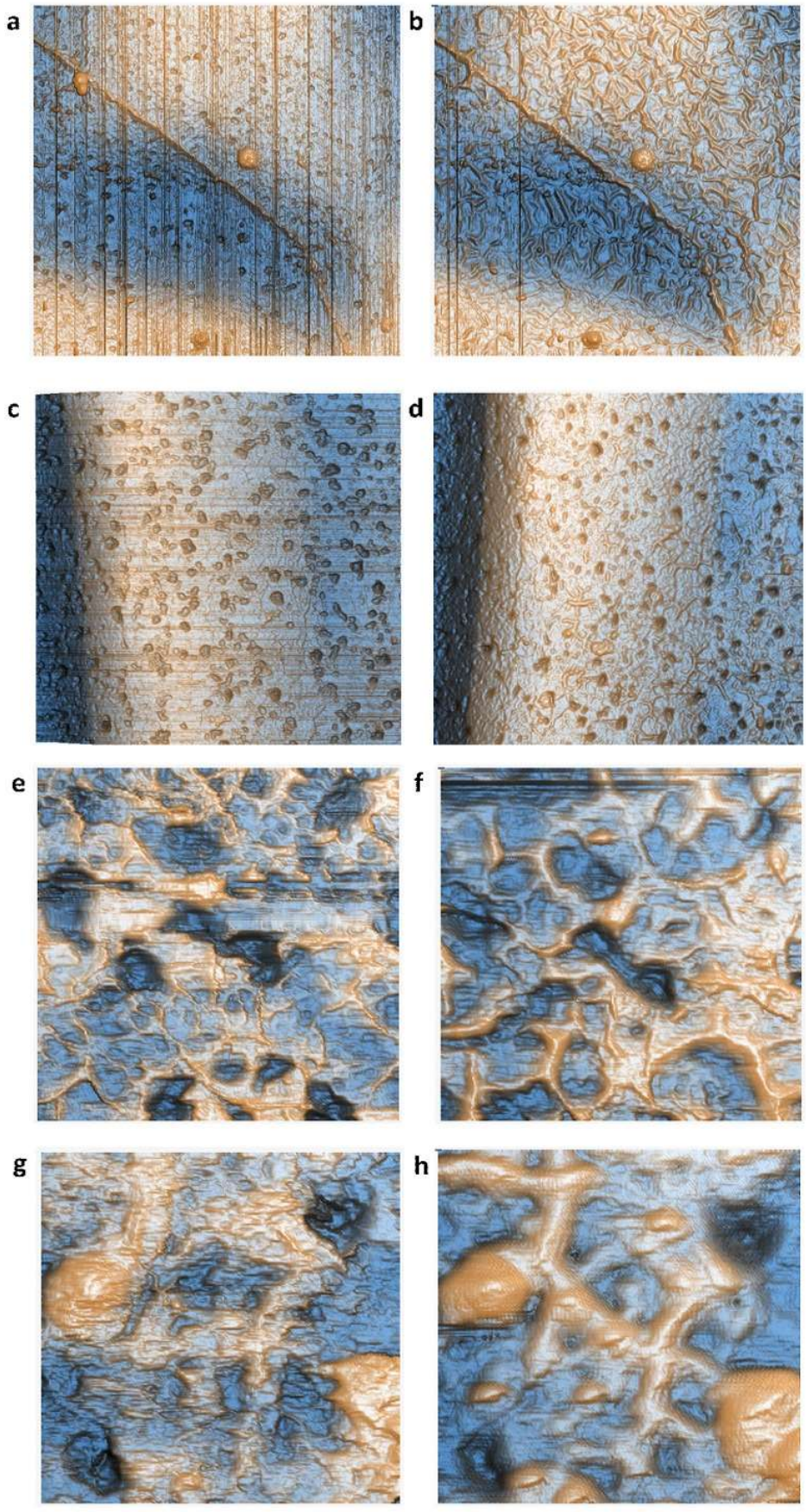

Figure S1. AFM analysis of the surface of carbon film/PMMA composites before UV treatments (a, c, e, g) and after UV dry treatment (b, f) and UV wet treatment (d, h). Vertical and horizontal lines are typical AFM artifacts (a-d: 10 x 10 µm, d-h: 1 x 1 µm).

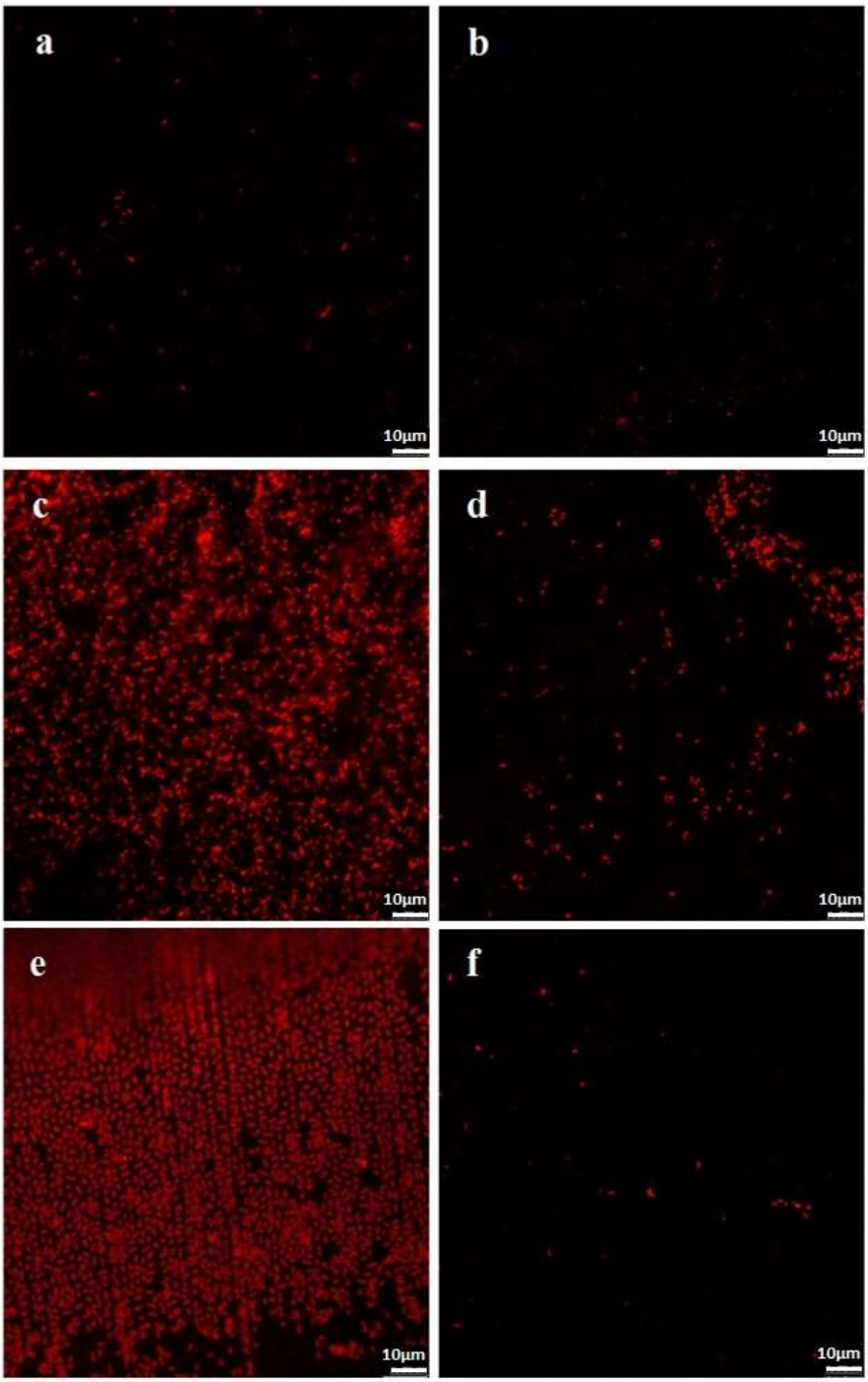

Figure S2. FilmTracer SYPRO Ruby staining revealing biofilm matrix for *E. coli* cultured on (a) glass-like carbon film as produced, (b) vacuum preconditioned film, (c) chamber-irradiated films in dry air, (d) chamber-irradiated films in wet air, (e) lamp-irradiated films in dry air and (f) lamp-irradiated films in wet air.